

# Observability analysis of relative localization for AUVs based on ranging and depth measurements

Gianluca Antonelli, Filippo Arrichiello, Stefano Chiaverini, Gaurav S. Sukhatme

**Abstract**—The paper studies the observability properties of the relative localization of two Autonomous Underwater Vehicles (AUVs) equipped with depth sensors, linear/angular velocity sensors, and communication devices with range measurement. The conditions that ensure observability of the linearized model and locally weak observability of the non-linear system are derived. An Extended Kalman Filter is then designed aimed at estimating the relative position between two AUVs. Simulations in 3D and reconstruction from experimental data in 2D provide a numerical validation of the analysis.

## I. INTRODUCTION

Absolute localization of Autonomous Underwater Vehicles (AUVs) is a non-trivial problem that usually requires the use of arrays of static transponders working as reference points. In this case, the localization can be achieved by means of triangulation-based techniques. The cost of deploying the transponders and calibrate them is, however, large and more effective techniques might be useful.

Despite the cooperative localization problem for generic robotic systems has been widely investigated in the last decade (see e.g. the papers in [5], [9], [15], [3]), the developed techniques can not be directly extended to the underwater scenario. Indeed, under the water it is not possible to use an internal sensor able to measure the position of the vehicle; moreover, due to the properties of the electromagnetic field, techniques such as GPSs (Global Positioning Systems) are not allowed too. An AUV is usually equipped with several sensors giving partial information about its state such as, e.g., accelerometer, depth sensor, compass, gyroscope, and Doppler velocity logger. Estimating the position of a moving body by measuring its derivatives, however, leads to the well known problem of integrating noise, i.e., the dynamic equations representing the errors are similar to the random walking system that is characterized by an increasing variance. In words, the error is not bounded. In [2] amplitudes of typical navigation errors with different kind of sensors are given; for example, vehicles relying on compass and speed estimation may have errors up to the 20% of the distance traveled.

Recently, acoustic modems became affordable instruments to allow communication of the underwater vehicles among themselves or with a surface boat; those instruments usually

allow measurements of the distance between transponder and receiver or between two modems. One example of a ranging measurement device is provided by [16] where the Woods Hole Oceanographic Institute (WHOI) micro-modem is presented.

A possible localization approach is based on the use of one vehicle with absolute position measurement capabilities (for example an autonomous surface vessel equipped with GPS) coordinating its motion with one or more underwater vehicles with ranging measurement capabilities. The underwater vehicles, thus, would be able to measure their absolute positioning without the need for a static baseline acoustic, and they would be able to enlarge the corresponding area limited to few square kilometers.

In [2] and [1], the same problem is afforded and effectively solved by building, at each sample time, all the possible solutions to the localization problem and selecting the most appropriate by minimizing a proper cost function. Outstanding experimental results are presented in different scenarios; moreover, the use of surface test vehicles equipped with GPS gives also ground truth data. The work [2], however, does not address observability issues. In the same paper the EKF (Extended Kalman Filter) is not used due to the possible presence of outliers in the measurements that, however, were not experienced in the given tests.

An observability analysis for differential drive mobile robots with various kind of relative measurements available is performed in [12]. The work [13] focuses on the aspects of cooperative decentralized localization with a Maximum A Posteriori estimator. The work [17] investigates the relative pose estimation based on range measurement between two robots moving in a 2D environment. Our work is strongly inspired by [17]; however, we take into account a 3D kinematic model instead of the 2D one, we consider a sensor suite customized for AUVs, and we present a non-linear observability analysis based on [8]. In our work, the AUVs are supposed to be equipped with a GPS that make them available their positioning when surfacing. Thus, supposing to start the mission with the AUVs on the surface, their initial relative positioning is known, and the filter can be properly initialized (differently from [17] where they develop an initialization procedure for the planar case).

Within a context of cooperative control of marine vehicles [4], in this paper we analyze the observability issues of the relative localization problem between Autonomous Underwater Vehicles (AUVs) equipped with depth sensors and communication devices with range measurement. In particular, we investigate the different kind of vehicles' relative

G. Antonelli, F. Arrichiello (corresponding author) and S. Chiaverini are with the Dipartimento di Automazione, Elettromagnetismo, Ingegneria dell'Informazione e Matematica Industriale, Università degli Studi di Cassino, Via G. Di Biasio 43, 03043, Cassino (FR), Italy, {antonelli, arrichiello, chiaverini}@unicas.it.

G.S. Sukhatme is with the Robotic Embedded Systems Laboratory, University of Southern California, Los Angeles, CA 90089, USA gaurav@usc.edu

movements that can eventually affect the observability of the non-linear and of its linearized model. A straightforward Extended Kalman Filter (EKF) is then designed aimed at estimating the relative position between two AUVs. Finally, numerical simulations in 3D and reconstruction from experimental data in a 2D case provide a numerical validation of the analysis.

## II. PROBLEM FORMULATION

Let  $\Sigma_I : \{O - \mathbf{x} \mathbf{y} \mathbf{z}\}$  be an inertial, earth-fixed, reference frame and let  $\Sigma_{v,i} : \{O_{v,i} - \mathbf{x}_{v,i} \mathbf{y}_{v,i} \mathbf{z}_{v,i}\}$  be the vehicle-fixed frame of the  $i^{th}$  vehicle. The unit vector  $\mathbf{z}$  is parallel to gravity,  $\mathbf{x}_{v,i}$  is parallel to the vehicle fore-aft direction, and  $\mathbf{z}_{v,i}$  is aligned with  $\mathbf{z}$  when the vehicle is neutrally leveled.

The kinematic equations representing the relative motion of one vehicle with respect to the other are given by

$$\dot{\mathbf{p}} = -\mathbf{v}_1 + \mathbf{R}_2^1 \mathbf{v}_2 - \mathbf{S}(\boldsymbol{\omega}_1) \mathbf{p} \quad (1)$$

where  $\mathbf{p} \in \mathbb{R}^3$  is the position of the second vehicle with respect to the first one expressed in frame  $\Sigma_{v,1}$ ; the vector  $\mathbf{v}_i \in \mathbb{R}^3$  (with  $i = \{1, 2\}$ ) is the linear velocity of the frame origin of  $\Sigma_{v,i}$  expressed in the same frame  $\Sigma_{v,i}$ ; the vector  $\boldsymbol{\omega}_1$  is the angular velocity of the frame  $\Sigma_{v,1}$  expressed in the same frame  $\Sigma_{v,1}$ ; the angular velocity tensor  $\mathbf{S}(\boldsymbol{\omega})$  (where  $\boldsymbol{\omega} \in \mathbb{R}^3 = [\omega_x \ \omega_y \ \omega_z]^T$ ) is defined as the skew symmetric matrix:

$$\mathbf{S}(\boldsymbol{\omega}) = \begin{bmatrix} 0 & -\omega_z & \omega_y \\ \omega_z & 0 & -\omega_x \\ -\omega_y & \omega_x & 0 \end{bmatrix} \quad (2)$$

and, finally, the matrix  $\mathbf{R}_2^1 \in \mathbb{R}^{3 \times 3}$  is the rotation matrix from frame  $\Sigma_{v,2}$  to frame  $\Sigma_{v,1}$ . Figure 1 illustrates the relationship among the variables above.

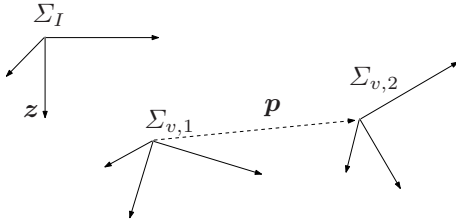


Fig. 1. Sketch of the main kinematic variables

Let assume an identical sensor suite on board each vehicle allowing to measure orientation, depth, linear and angular velocity. In addition, a ranging measurement is also available to the vehicles to measure their relative distance. It is required that one robot estimates the relative position of the second robot during their motion knowing its sensor information (linear/angular velocity, orientation and depth), the distance from the other robot, and the sensor information of the second robot (linear velocity, orientation and depth) received via underwater communication.

Denoting as  $\boldsymbol{\eta}_i \in \mathbb{R}^3 = [\eta_{i,x} \ \eta_{i,y} \ \eta_{i,z}]^T$  the coordinate of the origin of frame  $\Sigma_{v,i}$  in the inertial reference system  $\Sigma_I$ . We want to estimate the relative positioning of

vehicle 2 with respect to vehicle 1 from the output vector  $\mathbf{y} \in \mathbb{R}^2$  defined as:

$$\mathbf{y} = \begin{bmatrix} \frac{1}{2} \mathbf{p}^T \mathbf{p} \\ \eta_{2,z} - \eta_{1,z} \end{bmatrix}. \quad (3)$$

In particular, the depth difference  $\eta_{2,z} - \eta_{1,z}$  can be expressed in the frame  $\Sigma_{v,1}$  as  $\eta_{2,z} - \eta_{1,z} = [0 \ 0 \ 1] \mathbf{R}_1^I \mathbf{p}$ , where the matrix  $\mathbf{R}_1^I \in \mathbb{R}^{3 \times 3}$  represents the rotation from frame  $\Sigma_{v,1}$  to the inertial frame  $\Sigma_I$ . Thus, the output vector  $\mathbf{y}$  is modified into:

$$\mathbf{y} = \begin{bmatrix} \frac{1}{2} \mathbf{p}^T \mathbf{p} \\ [0 \ 0 \ 1] \mathbf{R}_1^I \mathbf{p} \end{bmatrix}. \quad (4)$$

It is worth noticing that, as in [17], we use the square distance instead of the distance itself as the first output element.

Defining as  $\mathbf{p}$  the system state, the following nonlinear continuous-time dynamic system is obtained from equations (1)-(4):

$$\begin{cases} \dot{\mathbf{p}} = \mathbf{f}(\mathbf{p}, \mathbf{u}) \\ \mathbf{y} = \mathbf{h}(\mathbf{p}) \end{cases} \quad (5)$$

for which an estimate  $\hat{\mathbf{p}}$  needs to be designed.

## III. OBSERVABILITY ANALYSIS

The system observability is at first discussed in terms of the linearized model, and then in terms of the non-linear observability, in particular by the property of local weak observability discussed in [8].

### A. Linearized model

The dynamic equations of the linearized model for a nominal input  $\mathbf{u} = \bar{\mathbf{u}}$  and a nominal state  $\mathbf{p} = \bar{\mathbf{p}}$  can be derived as:

$$\begin{cases} \delta \dot{\mathbf{p}} = \mathbf{A} \delta \mathbf{p} + \mathbf{B} \delta \mathbf{u} \\ \delta \mathbf{y} = \mathbf{C} \delta \mathbf{p} \end{cases} \quad (6)$$

where the dynamic matrix  $\mathbf{A} \in \mathbb{R}^{3 \times 3}$  is given by

$$\mathbf{A} = \left. \frac{\partial \mathbf{f}}{\partial \mathbf{p}} \right|_{\mathbf{u}=\bar{\mathbf{u}}, \mathbf{p}=\bar{\mathbf{p}}} = -\mathbf{S}(\bar{\boldsymbol{\omega}}_1) \quad (7)$$

and the output matrix  $\mathbf{C} \in \mathbb{R}^{2 \times 3}$  by

$$\mathbf{C} = \left. \frac{\partial \mathbf{h}}{\partial \mathbf{p}} \right|_{\mathbf{u}=\bar{\mathbf{u}}, \mathbf{p}=\bar{\mathbf{p}}} = \begin{bmatrix} \bar{\mathbf{p}}^T \\ \mathbf{z}_{v,1}^I{}^T \end{bmatrix} \quad (8)$$

where the following equality has been used:

$$\mathbf{z}_{v,1}^I{}^T = [0 \ 0 \ 1] \mathbf{R}_1^I. \quad (9)$$

It is worth noticing for the following derivations that the vector  $\mathbf{z}_{v,1}^I$  is not a function of the state  $\mathbf{p}$ .

The corresponding observability matrix  $\mathbf{O} \in \mathbb{R}^{6 \times 3}$  of the linearized system is given by

$$\mathbf{O} = \begin{bmatrix} \bar{\mathbf{p}}^T \\ \mathbf{z}_{v,1}^I{}^T \\ -\bar{\mathbf{p}}^T \mathbf{S}(\bar{\boldsymbol{\omega}}_1) \\ -\mathbf{z}_{v,1}^I{}^T \mathbf{S}(\bar{\boldsymbol{\omega}}_1) \\ \bar{\mathbf{p}}^T \mathbf{S}(\bar{\boldsymbol{\omega}}_1)^2 \\ \mathbf{z}_{v,1}^I{}^T \mathbf{S}(\bar{\boldsymbol{\omega}}_1)^2 \end{bmatrix}. \quad (10)$$

It is worth noticing that the observability matrix has at least rank 1; this rank condition is experienced if the vehicles are on the same vertical ( $\mathbf{p}||\mathbf{z}_{v,1}^I$ ) with null angular velocity. Assuming the vehicles are not aligned along the vertical direction is a necessary and sufficient condition to have at least rank equal two.

The first row of (10) represents the relative position, while the third one represents the cross product between the relative position vector and the angular velocity one. Obviously, if both  $\bar{\boldsymbol{\omega}}_1$  and  $\bar{\mathbf{p}}$  are different from the null vector, and they are not linearly dependent, then the first and third rows of the observability matrix are linearly independent. If, in addition,  $\bar{\boldsymbol{\omega}}_1$  is not orthogonal to the plane formed by the vectors  $\mathbf{z}_{v,1}^I$  and  $\bar{\mathbf{p}}$ , then the matrix has maximum rank, i.e.,  $\rho(\mathbf{O}) = 3$  where the symbol  $\rho$  denotes the rank operator.

Finally, let us customize the observations for a couple of AUVs traveling on two different horizontal planes with null pitch and roll angles ( $\mathbf{z}_{v,1}^I = [0 \ 0 \ 1]^T$ ), the only angular velocity component is  $\omega_{1,z}$  and thus the vector  $\boldsymbol{\omega}_1$  is parallel to  $[0 \ 0 \ 1]^T$ . If  $\omega_{1,z}$  is different from zero and if the vehicles are not aligned along the vertical direction, then  $\rho(\mathbf{O}) = 3$ . Thus, have a full rank  $\mathbf{O}$ , it seems to be necessary having a change in the yaw.

### B. Local weak observability

Given the non-linear system of eq. (5), more advanced mathematical tools aimed at studying the observability for non-linear systems may be required, such as the concept of *local weak observability* introduced in [8]. The reader may consider the synthetic overview of the concepts of observability, Lie derivatives and observability rank condition given within a context of relative localization in [17].

By defining the Lie derivatives of the scalar output  $h_j$  as

$$\mathcal{L}_f^0 h_j = h_j \quad (11)$$

$$\mathcal{L}_f^1 h_j = \nabla h_j \cdot \mathbf{f} = \frac{\partial h_j}{\partial \mathbf{p}} \cdot \mathbf{f} = \sum_{i=1}^3 \frac{\partial h_j}{\partial p_i} \cdot f_i \quad (12)$$

$$\mathcal{L}_f^2 h_j = \frac{\partial}{\partial \mathbf{p}} [\mathcal{L}_f^1 h_j] \cdot \mathbf{f} \quad (13)$$

$$\dots \quad (14)$$

$$\mathcal{L}_f^n h_j = \frac{\partial}{\partial \mathbf{p}} [\mathcal{L}_f^{n-1} h_j] \cdot \mathbf{f} \quad (15)$$

it is possible to define the observability matrix as the matrix with an infinite number of rows defined as

$$\mathbf{O} = \begin{bmatrix} \nabla \mathcal{L}_f^0 h_1 \\ \nabla \mathcal{L}_f^0 h_2 \\ \nabla \mathcal{L}_f^1 h_1 \\ \nabla \mathcal{L}_f^1 h_2 \\ \vdots \\ \nabla \mathcal{L}_f^n h_1 \\ \nabla \mathcal{L}_f^n h_2 \end{bmatrix} \quad (16)$$

with  $n \in \mathbb{N}$ . The matrix  $\mathbf{O}$  for the problem at hand becomes

$$\mathbf{O} = \begin{bmatrix} \mathbf{p}^T \\ \mathbf{z}_{v,1}^{I \ T} \\ [-\mathbf{v}_1 + \mathbf{R}_2^1 \mathbf{v}_2]^T \\ -\mathbf{z}_{v,1}^{I \ T} \mathbf{S}(\boldsymbol{\omega}_1) \\ [-(\mathbf{v}_1 + \mathbf{R}_2^1 \mathbf{v}_2) \mathbf{S}(\boldsymbol{\omega}_1)]^T \\ \mathbf{z}_{v,1}^{I \ T} \mathbf{S}(\boldsymbol{\omega}_1)^2 \\ \vdots \end{bmatrix}. \quad (17)$$

It can be demonstrated that higher order Lie derivatives are not useful to eventually increase the rank of  $\mathbf{O}$ .

It is also interesting to rewrite the matrix  $\mathbf{O}$  when the vehicle labeled as 1 has null pitch and roll angles, in such a case, in fact, it holds  $\mathbf{z}_{v,1}^I = [0 \ 0 \ 1]^T$  and the second measurement is  $p_z$ , thus:

$$\mathbf{O} = \begin{bmatrix} [\mathbf{p}^T] \\ 0 \quad 0 \quad 1 \\ [-\mathbf{v}_1 + \mathbf{R}_2^1 \mathbf{v}_2]^T \\ \omega_{1,y} \quad -\omega_{1,x} \quad 0 \\ [-(\mathbf{v}_1 + \mathbf{R}_2^1 \mathbf{v}_2) \mathbf{S}(\boldsymbol{\omega}_1)]^T \\ \omega_{1,x} \omega_{1,z} \quad \omega_{1,y} \omega_{1,z} \quad -\omega_{1,x}^2 - \omega_{1,y}^2 \\ \vdots \end{bmatrix}. \quad (18)$$

One interesting difference with respect to the linearized model is given by the presence of the linear velocity in the matrix  $\mathbf{O}$ . This gives an additional possibilities to try to achieve observable configurations by properly selecting the inputs. Moreover, by visual inspection of the first three rows it is already possible to find a sufficient condition to ensure the local weak observability property. The third line represent the velocity of the second vehicle, *as seen from the first vehicle*, expressed in the frame of the first vehicle. It is sufficient that this relative velocity is not a linear combination of  $z_I$  and  $\mathbf{p}$ . Differently from the previous case, thus, a local weak observability can be achieved without inspecting the angular velocities that can be eventually null.

By including in the discussion the angular velocity it can be easily verified, for example, that a non-null component of the  $\boldsymbol{\omega}$  vector in the orthogonal direction to the  $z_I$ - $\mathbf{p}$  plane may give full rank.

## IV. OBSERVER DESIGN

It is of interest to design an observer for  $\mathbf{p}$ , whose output, the estimate of the relative position, will be denoted as  $\hat{\mathbf{p}} \in \mathbb{R}^3$ . The local weak observability property introduced in [8] does not lead to an automatic design of such an observer. In the literature, several nonlinear observers have been proposed [7]; among them, one seminal result is given by the work of Isidori [10]. It is unlikely that this approach can be used in this case since it requires an invertible state transformation that gives a linear mapping in the output variable. In this case, since the measurement is the distance it seems that it is not possible to found an invertible mapping to the current state, i.e., the Cartesian coordinates.

One possible alternative would be the use of the Extended Luenberger observer; this approach, however, is based on the

linearized model and requires to solve a pole placement problem at each iteration that, in turn, requires full observability of  $A, C$  to compute the gain. Since the pole placement is usually achieved by the use of the Ackerman formula that requires the inversion of the observability matrix, this method is sensitive to *local* unobservable configurations. The latter are not rare for the AUVs case as discussed in Sect. III-A.

#### A. Extended Kalman Filter

One possible, systematic, observer design method is given by the use of the Extended Kalman Filter (EKF), and this is solution we adopt in this paper; however, it would be also possible use different kinds of filters like a particle filter or an Unscented Kalman Filter. The generic equations of an EKF are given by [6]:

$$\begin{cases} \dot{\hat{p}} &= f(\hat{p}, u) + K(y - h(\hat{p})) \\ K &= PC^T R_v^{-1} \\ \dot{P} &= AP + PA^T + R_w - PC^T R_v^{-1} CP \end{cases} \quad (19)$$

where  $R_v \in \mathbb{R}^{2 \times 2}$  and  $R_w \in \mathbb{R}^{3 \times 3}$  are the covariance matrices of the measurement and process noise, respectively, and  $K \in \mathbb{R}^{3 \times 2}$  is the gain matrix. Notice that, as derived in eq. (8), the matrix  $C$  is a function of the state computed at the current estimate, i.e.,  $C = C(\hat{p})$ .

There is no guarantee that the error  $p - \hat{p}$  converge to zero except if the initial condition are close to the true value and the linearized system is observable [14], [11].

It is known that this formulation of the EKF is the *optimum* filter only for Gaussian noises; according to [2] the ranging measurement provided by the WHOI micro-modem [16] can be model as a non-polarized stochastic variables with constant variance. In addition, depth sensors are usually affordable and satisfy the Gaussian assumption.

It is also of interest investigating the structure of the gain matrix for the specific case of the vehicle labeled as 1 with null pitch angle and roll angles. Given the fact that the two sensors are uncorrelated and assuming a diagonal  $R_v$  matrix, by observing the output matrix of the linearized model  $C$  it is possible to compute the following structure for the gain:

$$K = \begin{bmatrix} \star & 0 \\ \star & 0 \\ \star & \star \end{bmatrix}, \quad (20)$$

where the symbol  $\star$  denotes a value generically different from zero. This confirms the intuition of [2] in working on a planar model.

### V. NUMERICAL VALIDATION

In order to validate the proposed analysis, and to test the EKF filter performance, we present two different kinds of numerical evaluations. In the first one we present a set of numerical simulations executed in the Matlab environment to test the performance of the EKF in a 3D case. In the second one we use real data taken from two autonomous surface vessels (equipped with GPS, accelerometers and compass) to make an off-line testing of the EKF in a 2D case.

#### A. 3D numerical validation

In this section we present the results of the numerical simulations executed in the Matlab environment to test the EKF performance in the 3D space. In the considered example, one robot, moving in the 3D space changing its Roll, Pitch and Yaw (RPY) angles, has to estimate the relative position of a second robot via the filter of eq. (19). To this aim, the robot needs information from its onboard sensors (as linear/angular velocity, orientation, depth), information received from the other robot (about its velocity and depth expressed in the first robot inertial reference frame) and the relative distance between the two robot (that can measured by the time needed to send a message and receive an acknowledgement via the acoustic communication channel).

The main issues while choosing trajectories are related to the observability properties of the system described in the previous section. A deeper analysis of how to chose trajectories to ensure observability goes beyond the scope of this paper and it will be discussed in a different work. In this paper we use trajectories rich enough to make the system observable.

In order to simulate noises of realistic sensors, a random error with gaussian probability distribution and a standard deviation of 10 cm has been added to the range measurement; moreover, a random error with gaussian probability distribution and a standard deviation of 10 cm has been added to the depth sensor measurement. The initial value of the EKF parameters have been chose by trial and error as:

$$P = 10^{-3} I_3; \quad R_v = \begin{bmatrix} .2 & 0 \\ 0 & .1 \end{bmatrix}; \quad R_w = .2 I_3,$$

where  $I_n \in \mathbb{R}^{n \times n}$  is an n-dimensional identity matrix.

Figures 2-4 show the results of a simulation where we have supposed that an initial measurement of the relative position of the robots is available; that means, we have chosen a null initial estimate error for the filter. In particular, figure 2 shows the path of the first robot (the blue closed trajectory), the path of the second robot (the red trajectory) and the estimate of the position of the second robot done by the first one (the green path). Figure 3 respectively shows the measured distance between the robots and their depth difference. Figure 4 shows the filter estimation error; it is worth noticing that, despite the estimation error is not exactly null, the filter is stable and the error is lower than 10 cm when the vehicles has a relative distance in the range of 30 – 55 m.

The assumption of having an initial estimate of the robot positions is reasonable for a large class of the underwater vehicles. These robots, in fact, are usually equipped with GPS that gives the positioning when the robot are surfacing. Thus, it reasonable assuming that a mission starts with the robots at the sea surface. However, to test the behavior of the system when the initial estimate is not exactly known, we have performed a second simulation where the robot execute the same path of the previous mission but the estimate of the EKF has an initial error of about 17 m ( $[10 \ 10 \ 10]$  m). Figure 5-6 respectively show the robot/estimate paths and the estimation error while executing the mission. It is worth



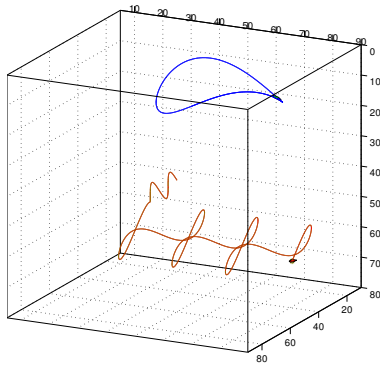


Fig. 2. Paths followed by the two robots (blue and red paths) and the estimated position of one robot as seen by the other (green path). The initial error of the EKF is supposed null.

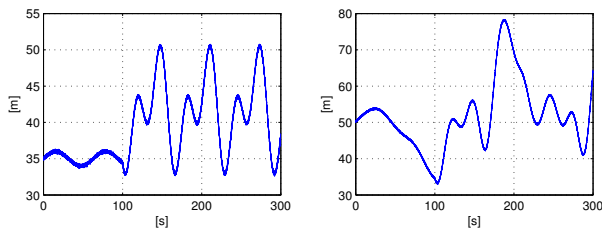


Fig. 3. Distance (left plot) and depth difference (right plot) between the robots during the first numerical simulation.

noticing that filter quickly reduces the estimation error and keeps the same error magnitude of the previous case.

### B. 2D validation using boats' sensor data

For the second numerical evaluation we have used real data take from sensors of two autonomous surface vessels and we have done an off-line analysis of the filter in the 2D case. The used robotic platform (see fig 7) is composed by two Autonomous Surface Vessels (ASVs) designed by the University of Southern California's Robotic Embedded Systems Lab. Each ASV has a sensor suite consisting of a science package used to gather weather, bathymetry, and water chemistry data, and a navigation package consisting of a Microstrain 3DMG Inertial Measurement Unit (IMU), a uBlox GPS unit, and a Crossbow Dynamic Measurement Unit (DMU). The 3DMG IMU is used as a compass and a 3-axis accelerometer generating measurements at 32 Hz, the uBlox GPS provides global position at 1 Hz, and the Crossbow DMU serves as a rate gyro with a sampling rate of 120 Hz. To take the data we driven the boats via the remote controllers and we used the on-board systems to store data from the different sensors and to synchronize them for post-processing. In particular, we used data from GPS, compass and Rate Gyro to extrapolate the data for the EKF (the range measurement is calculated by the GPS positioning).

For the proposed case we used a static version of the EKF ( $\dot{P} = 0$ ) and we select the gains as  $P = 10I_2$ ;  $R_v = 1000$ .

Figure 8 shows the paths of the vessels and of their position as estimated by the other vessel; in particular, the red

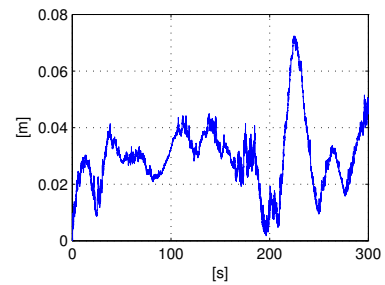


Fig. 4. Estimation error of the EKF during the first numerical simulation.

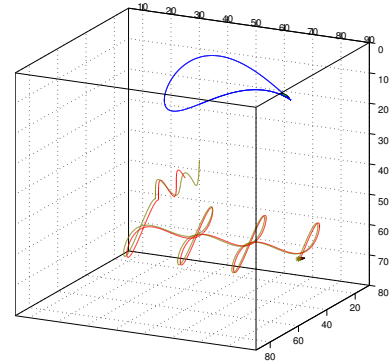


Fig. 5. Paths followed by the two robots (blue and red paths) and the estimated position of one robot as seen by the other (green path). The initial error of the EKF is of 17 m.

and the blue paths represent the paths of the two robots, while the green and the black represent the estimated positions. Despite sensor noises and non linearities, the estimation error is lower than 10 m (as shown in figures 9) while the vessels have a relative distance of the order of 100 m. It is worth noticing that the error peaks are related to low-velocity maneuver when the vessels make small radius turns. Moreover the approach seems to be numerically sensitive to the inter-vehicle distances.

## VI. CONCLUSIONS

This paper focuses on the relative position estimation problem for two underwater robots that can not measure their absolute positioning except when they are at the sea surface level. We assume, instead, that the robots have onboard sensor to measure their state, and that they can communicate via acoustic underwater modems. Moreover, from the time shift between the sent and received messages, the modems are able to measure the relative distance between the two robots. Using on these information, we have studied the observability properties of the non-linear system composed by the two robots when the output is given by depth and range measurement. We have firstly studied the observability properties of the linearized system and then the locally weak observability properties of the non-linear system. Then, we have developed an Extend Kalman Filter and we have numerically tested its performances both in a 3D case via simulation and in a 2D case via off-line analysis starting from

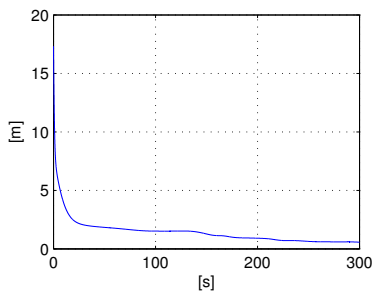


Fig. 6. Estimation error of the EKF during the second numerical simulation.



Fig. 7. The USC RESL Autonomous Surface Vehicle used for the experiments reported here.

real sensor information. The results prove the effectiveness of the proposed analysis.

Future works will focus on the study of how to integrate the filters on each robot to increase their global performances; moreover, we will study the extension of the proposed technique to more than two robots. Finally, we will study the impact of multi-path effects, outliers and transmission delays of the under-water acoustic communication on the relative positioning estimation.

#### ACKNOWLEDGMENTS

The research leading to these results has received funding from the European Community's Seventh Framework Programme under grant agreement n. 231378 (STREP project Co<sup>3</sup>AUVs - Cognitive Cooperative Control for Autonomous Underwater Vehicles). This work was supported in part by the NOAA MERHAB program under grant NA05NOS4781228 and by NSF as part of the Center for Embedded Network Sensing (CENS) under grant CCR-0120778, by NSF grants CNS-0520305 and CNS-0540420, by the ONR MURI program (grants N00014-09-1-1031 and N00014-08-1-0693) by the ONR SoA program and a gift from the Okawa Foundation.

#### REFERENCES

- [1] A. Bahr. *Cooperative localization for autonomous underwater vehicles*. PhD thesis, Massachusetts Institute of Technology & Woods Hole Oceanographic Institution, 2008.
- [2] A. Bahr, J.J. Leonard, and M.F. Fallon. Cooperative localization for autonomous underwater vehicles. *The International Journal Robotics Research*, 28:714–728, June 2009.
- [3] P. Batista, C. Silvestre, and P. Oliveira. Necessary and sufficient conditions for the observability of linear motion quantities in strap-down navigation systems. In *Proceedings of 2009 American Control Conference*, pages 1177–1182, St. Louis, MO, USA, 2009.
- [4] A. Birk, G. Antonelli, A. Pascoal, and A. Caffaz. Cognitive cooperative control for autonomous underwater vehicles. In *Proceedings 8th International Conference on Computer and IT Applications in the Maritime Industries, COMPIT'09*, pages 136–149, Budapest, Hungary, May 2009.

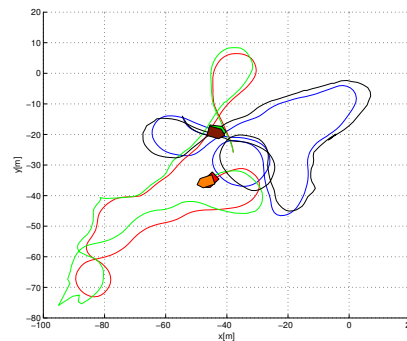


Fig. 8. Paths of the vessels and of their positions as estimated by the neighboring robots; the red and blue paths are the paths of the two robots, the green and black are the estimated positions.

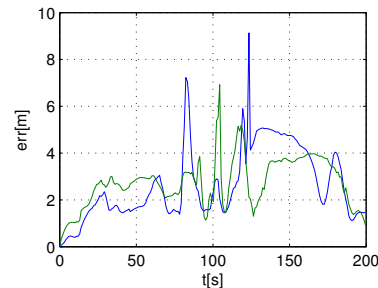


Fig. 9. Error of the relative estimations.

- [5] D. Fox, W. Burgard, and S. Thrun. A probabilistic approach to collaborative multi-robot localization. *Autonomous Robots*, 8(3):325–344, June 2002.
- [6] A. Gelb. *Applied Optimal Estimation*. M.I.T. Press, M, 1990.
- [7] J. Hedrick and A. Girardi. *Control of Nonlinear Dynamic Systems: Theory and Applications*. University of California, 2005.
- [8] R. Hermann and A. Krener. Nonlinear controllability and observability. *IEEE Transactions on Automatic Control*, 22(5):728–740, 1977.
- [9] A. Howard, MJ Mataric, and GS Sukhatme. Putting the 'I' in 'team': an ego-centric approach to cooperative localization. In *Proceedings of 2003 IEEE International Conference on Robotics and Automation*, volume 1, 2003.
- [10] A. Isidori. *Nonlinear control systems: an introduction*. Springer Verlag, 1995.
- [11] A.J. Krener. The convergence of the extended Kalman filter. *Lecture Notes in Control and Information Sciences*, pages 173–182, 2003.
- [12] A. Martinelli and R. Siegwart. Observability analysis for mobile robot localization. In *Proceedings IEEE/RSJ International Conference on Intelligent Robots and Systems*, pages 1471–1476, 2005.
- [13] E.D. Nerurkar, S.I. Roumeliotis, and A. Martinelli. Distributed maximum a posteriori estimation for multi-robot cooperative localization. In *Proceedings 2009 IEEE International Conference on Robotics and Automation*, pages 1402–1409, Kobe, J, May 2009.
- [14] K. Reif, S. Gunther, E. Yaz, and R. Unbehauen. Stochastic stability of the discrete-time extended Kalman filter. *Automatic Control, IEEE Transactions on*, 44(4):714–728, Apr 1999.
- [15] S. Roumeliotis and G. Bekey. Distributed multirobot localization. *IEEE Transactions on Robotics and Automation*, 18(5):781–795, 2002.
- [16] S. Singh, M. Grund, B. Bingham, R. Eustice, H. Singh, and L. Freitag. Underwater acoustic navigation with the WHOI micro-modem. In *Proceedings MTS/IEEE Conference and Exhibition OCEANS 2000*, 2000.
- [17] X.S. Zhou and S.I. Roumeliotis. Robot-to-robot relative pose estimation from range measurements. *IEEE Transactions on Robotics*, 24(6):1379–1393, Dec. 2008.